*29th EPS Conference on Plasma Phys. and Contr. Fusion Montreux, 17-21 June 2002 ECA Vol. **26B**, P-2.063 (2002)*

ELECTRON TRANSPORT BARRIERS IN TEXTOR PLASMAS

R. Jaspers[1], G.M.D. Hogeweij[1], A. Merkulov[1], E.Westerhof[1], F.C. Schüller[1], H.R. Koslowski[2], A.M. Messiaen[3]

Trilateral Euregio Cluster (TEC):
[1]FOM-Instituut voor Plasmafysica 'Rijnhuizen', Associatie EURATOM-FOM, P.O. Box 1207, 3430 BE Nieuwegein, The Netherlands
[2]Institut für Plasmaphysik, Association EURATOM-FZ Jülich, D-52425 Jülich, Germany
[3]Lab. de Physique des Plasmas, ERM-KMS, Association EURATOM-Belgian State, Brussels, Belgium

1. Introduction

The outstanding result from the now dismantled tokamak RTP was the observation that the electron heat conductivity is layered as evidenced by the presence multiple electron transport barriers located near low order rational values of the safety factor q [1]. These results were explained by the so-called q-comb model for the electron heat conductivity, χ_e, in which χ_e is supposed to be a function of q only with a constant high value interspersed with narrow regions of low conductivity located near the low rational values of q: 1, 4/3, 3/2, 2, 5/2, 3, 7/2 … Similar experiments are now performed on a larger tokamak, TEXTOR, where contrary to RTP, the electron heating by ECRH is not the dominant heat source and the electrons are not completely decoupled from the ions.

The aim of these experiments is threefold: a) test whether the q-comb model under these different conditions still gives a consistent description for the electron heat transport, b) try to establish a large internal transport barrier, which is according to the q-comb model expected in a region with low magnetic shear close to rational q-values and c) study the electron transport under conditions of improved (ion) confinement.

2. Electron transport barriers in current flat top phase

As reported previously [2] for ohmic target discharges in TEXTOR centrally heated by 0.25 MW of ECRH (Ohmic heating 0.35 MW), the q-comb model works surprisingly well. When the absolute values of the heat conductivity are scaled by a factor 0.83 consistent with L-mode scaling between RTP and TEXTOR, the RTP model also describes well TEXTOR discharges with central ECRH. In fact, the inner most barrier near q = 1 is clearly visible in electron temperature profile as measured with high resolution Thomson Scattering and shown in Fig. 1.

The central barrier near q = 1 is confirmed by scanning the ECRH deposition through the plasma. Fig 2a shows the change in central temperature when the barrier is crossed. For higher current the position of the barrier is at larger radius as expected from the larger q=1 radius. The relation between the barrier and q=1 is further confirmed by the sawtooth behaviour. The inversion radius is close to the barrier position. Moreover for ohmic discharges the sawtooth

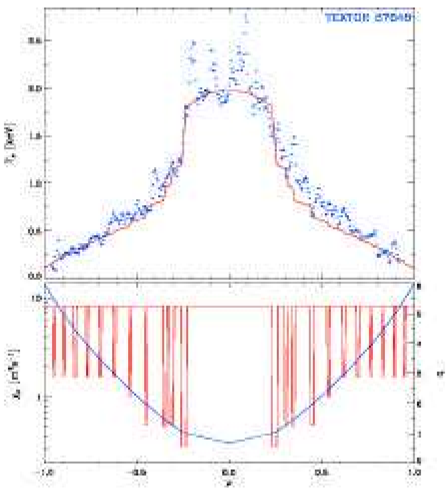

Fig. 1 The T_e profile in a typical TEXTOR discharge with central 250 kW ECRH simulated with the RTP q-comb model for the electron heat conductivity. Blue dots represent measured T_e. The red curve gives the result of the simulation. The bottom panel shows the q profile (blue) and the corresponding profile of the electron heat conductivity χ_e.

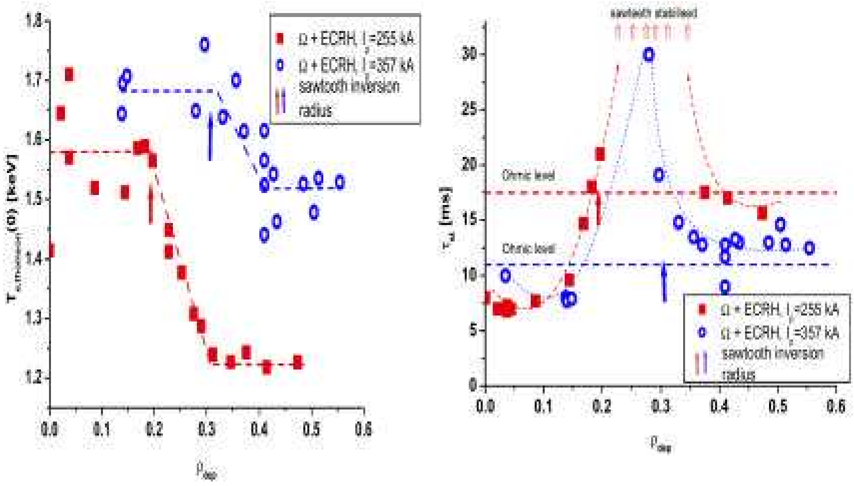

Fig. 2 The central T_e and the corresponding sawtooth period achieved in Ohmic discharges with ECRH as a function of the ECRH deposition radius. The ECRH deposition radius is varied by changing the toroidal field. Two datasets are shown: squares for I_p=255 kA and circles for 357 kA. In the lower current case sawteeth are stabilised, when ECRH is deposited within a region just outside the sawtooth inversion radius.

period has a marked maximum when ECRH is deposited close to the barrier and the sawtooth inversion radius (see Fig. 2b). For the lower current case, sawteeth are stabilised during the ECRH pulse when the power is deposited in a relatively broad region outside the inversion radius. There is no observation of a density pump out upon application of ECRH when the sawteeth are stabilised. Once sawteeth are stabilised by off-axis ECRH, the discharge remains in a non-sawtoothing regime after switch-off of ECRH. This behaviour is depicted in Fig. 3 representing the central SXR emission for different EC deposition radii. The enhanced SXR emission after the heating phase in these cases is mainly due to a density and impurity effect, since T_e before and after ECRH is comparable. For heating at or just outside the inversion radius a crash is observed after which the discharge returns to the normal sawtoothing regime.

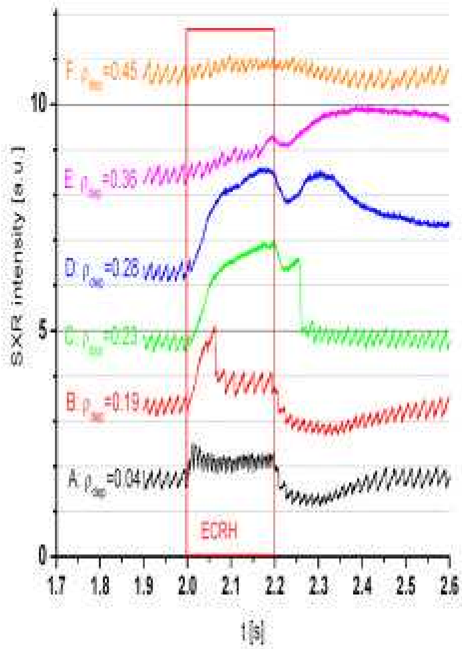

Fig. 3: Time traces of the SXR intensity for discharges differing in EC deposition radius. For central deposition (A) the sawteeth period is shortened. For heating outside the inversion radius (C-E) sawteeth are stabilised. The discharges remain in the non-sawteething regime even after switch off of ECRH. For D and E the SXR intensity is about a factor of 2 higher than in the ohmic case before ECRH. Note the crashes in B and C after which the discharges return to the normal sawtoothing regime.

3. ECRH during the current ramp phase

Given that the electron heat conductivity displays barriers near rational values of q, it is attractive to control the current density profile in such a way as to make optimal use of these barriers. One way to optimise the q profile is by creating low or negative central shear (NCS), i.e a hollow current density profile. This was tried at TEXTOR by means of early neutral beam heating during the current rise phase of the discharge: an increased temperature slows down current penetration, resulting in a hollow current profile. In the experiments, a fast initial ramp (100 ms) up to I_p = 200 kA is followed by a slower ramp up to 350 kA at t= 600 ms. Early heating is provided by 1.5 MW of counter-NBI from t = 200 ms. In addition to providing the required plasma heating a central counter driven current is expected to assist in attainment of NCS. Somewhat later ECRH (270 kW, t = 250 – 450 ms) is applied for additional electron heating to establish the presence of electron transport barriers. At t= 0.35 s, the electron temperature profile is measured by Thomson Scattering. The T_e profiles for different positions of ECRH deposition are shown in Fig. 4. Two transport barriers are identified in these profiles at normalised minor radii of ρ = 0.13 and 0.35.

At the beginning of the ECRH pulse the q-profile (as measured by polarimetry and confirmed by current diffusion calculations) is slightly reversed or flat with a central value of about 2 to 2.5. With central ECRH, regular sawteeth appear close to the end or shortly after ECRH. In normal discharges without early heating, sawteeth generally appear only much later. This indicates a strong evolution of the current density profile in the phase with central ECRH: in spite of the higher temperature, the strong central peaking of the T_e profile leads to a faster central current penetration, because of the reduced gradient length. This is confirmed by

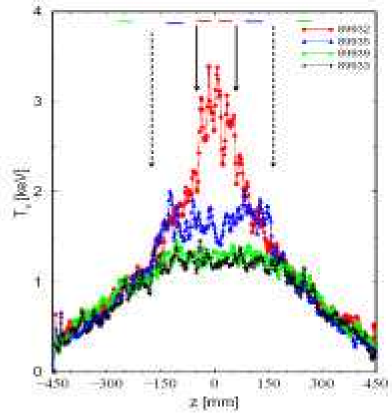

Fig. 4: T_e profiles from Thomson scattering at t=0.35s for different positions of ECRH deposition: 89932 ρ_{dep}=0.06; 89935 ρ_{dep} =0.23; 89939 ρ_{dep}=0.50; 89933 NBI-only.

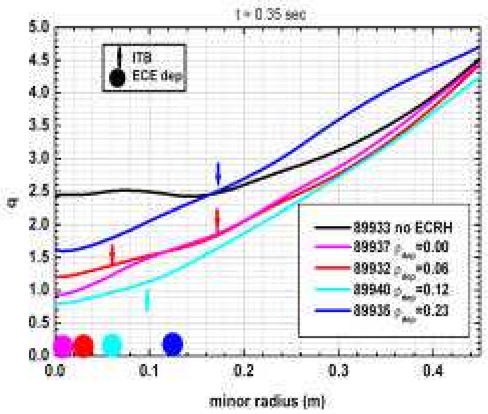

Fig. 5: q profiles as calculated with the ASTRA code at the time of Thomson Scattering. Observed barriers are indicated by arrows and are close to rational q-values: q=1,1.5,2,2.5. Note that central shear is not negative..

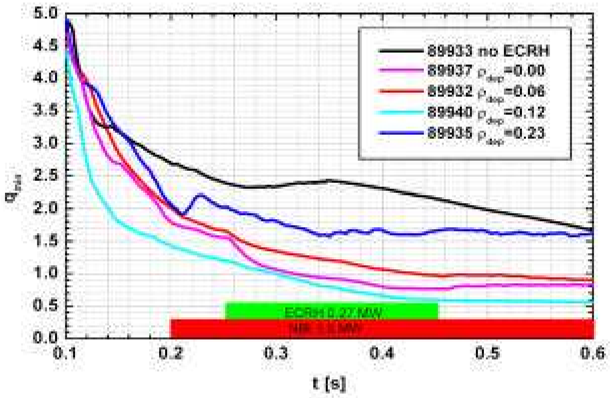

Fig. 6 The evolution of the minimal safety factor for discharges with different location of the ECR heating. The time at which q_0 =1 drops below 1 is qualitatively consistent with appearance of sawteeth.

calculations of the current penetration using the experimental T_e profile with neoclassical conductivity and an estimate of the beam driven current. From this type of calculation it was inferred that barriers in the T_e profile corresponded to q=1, 1.5, 2 and 2.5 for different ECRH deposition (Fig. 5). An independent check of these calculations was provided by the relation of the appearance of sawteeth in the experiment and the time the q_0 crossed the q=1 level (see Fig 6).

Apart from providing the necessary pre-heating, counter-NBI also proved essential for stability during central ECRH. Without NBI, ECRH in the current ramp phase is accompanied by one or more strong core collapses. Core collapses are also observed

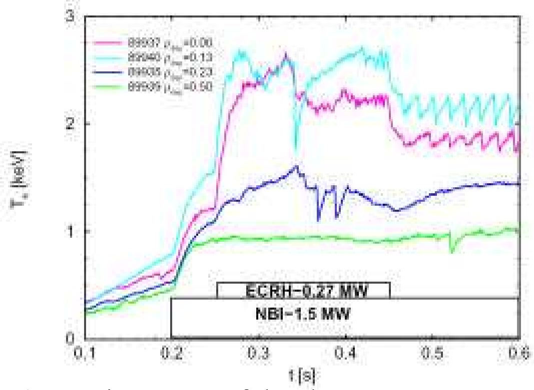

Fig. 7: Time traces of the electron temperature for various ECR heated discharges, with different deposition: 89937: ρ_{dep}=0.0, 89940 ρ_{dep}=0.13, 89935: ρ_{dep}=0.23 and 89939: ρ_{dep}=0.50. Note the large crash for 89940 and the appearance of sawteeth for rather centrally heated discharges and the absence of them for off-axis heating. The crashes in 89935 are most probably caused by MHD activity at q=1.5.

with off-axis ECRH as seen in the central T_e evolution (Fig. 7). A particularly strong core collapse is observed in the case where EC deposition coincides with the inner barrier (discharge 89940). Since the calculated q-profile shows at that time already q_0 smaller than 1, this is interpreted as a monster sawtooth. The subsequent stabilisation of the sawtooth is consistent with results from Fig 2b, where heating close to the inversion radius also suppressed the sawteeth.

4. ECRH in the Radiatively Improved mode

On TEXTOR a regime with improved confinement, Radiatively Improved mode or RI-mode, has been established by injection of radiating species in the plasma edge (typically Ne or Ar) [3]. Apart from a radiating mantle, this regime is characterised by establishment of a peaked density profile with a possible suppression of ion temperature gradient (ITG) turbulence as a consequence. The energy confinement in RI-mode scales with line averaged density $<n_e>$ as in the linear Ohmic confinement regime, but the general degradation of confinement with total heating power remains [3]: $\tau_{RI} \propto <n_e> P_{tot}^{-2/3} I_p$ (1)

The improvement of confinement is attributed to the suppression of the ITG turbulence, which is a major cause of anomalous ion heat conductivity. The electron heat conductivity and its improvement in RI-mode are less well known. It is thus of particular interest to study pure electron heating as provided by ECRH. However, the 200 ms pulse length and 270 kW injected power of the preliminary 110 GHz system are limited when compared to confinement times of about 50 ms and the total heating power of about 2.7 MW of typical RI-mode discharges. Still, interesting results have been obtained on ECRH in RI-mode.

Results for a typical RI-mode discharge with central ECRH are shown in Fig. 8, which gives normalised efficacy $(\delta W_{dia}/W_{dia}) / (\delta P/P_{tot})$ as a function of ECRH deposition radius. Two interesting observations are made: a) although not as sharp as in the ohmic phase, the features of a transport barrier in the region around the sawtooth inversion radius can be recognized and b) for heating inside this transport barrier no power degradation is noticed. Moreover, during ECRH the density continues to rise: no pump-out is observed with ECRH in RI-mode.

5. Conclusions

The electron transport in ECR heated TEXTOR discharges are compatible with the q-comb model. A clear q=1 barrier was observed. Heating just outside the barrier stabilised the sawteeth. By heating in the current ramp phase several electron internal barriers could be distinguished, all related to rational values in the q-profile. These profiles were calculated from the current diffusion taking into account bootstrap and NBI driven current.

In RI-mode discharges a q=1 barrier was found as well. Heating with ECRH inside this barrier did not show any power degradation.

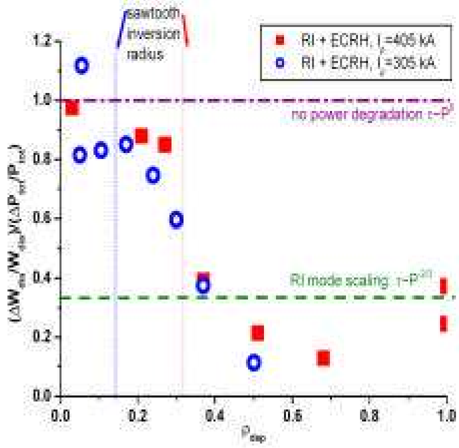

Fig. 8: Normalised efficacy of ECRH in RI-mode discharges for two different currents. A transport barrier close to the inversion radius might be recognized. For heating inside this transport barrier no power degradation is observed.

References

[1] N.J. Lopes Cardozo et al., Plasma Phys. Control. Fusion **39** (1997) B303.

[2] F.C.Schüller et al., 27th EPS Conf. On Contr. Fusion and Plasma Physics, Budapest (2000) http://epsppd.epfl.ch/Buda/pdf/d1_002.pdf

[3] R.R.Weynants et al., Nucl. Fusion **39** (1999) 1637.